IJNAOE
©SNAK, 2015

Int. J. Nav. Archit. Ocean Eng. (2015) 7:409~425
http://dx.doi.org/10.1515/ijnaoe-2015-0029
pISSN: 2092-6782, eISSN: 2092-6790

Dynamics modeling of a semi-submersible autonomous underwater vehicle with a towfish towed by a cable

Jinmo Park and Nakwan Kim

Department of Naval Architecture and Ocean Engineering, Seoul National University, Seoul, Korea

ABSTRACT: *In this paper, we employ a dynamics modeling method for investigating a multi-body dynamics system of semi-submersible autonomous underwater vehicles consisting of a towing vehicle operated near the water surface, a tow cable, and a towfish. The towfish, which is towed by a marine cable for the purposes of exploration or mine hunting, is modeled with a Six-Degree-of-Freedom (6-DOF) equation of motion that reflects its hydrodynamics characteristics. The towing cable, which can experience large displacements and deformations, is modeled using an absolute nodal coordinate formulation. To reflect the hydrodynamic characteristics of the cable during motion, the hydrodynamic force due to added mass and the drag force are imposed. To verify the completeness of the modeling, a few simple numerical simulations were conducted, and the results confirm the physical plausibility of the model.*

KEY WORDS: Absolute nodal coordinate formulation; Flexible cable dynamics; Multi-body dynamics; Large deformation; Semi-submersible AUV; Towed system.

INTORODUCTION

Because the need for subsea exploration for discovery of subsea resources and for military purposes such as mine hunting is increasing, studies of marine cable motion and the use of towfish have been performed by many researchers. Most previous studies on these subjects were focused on a system that consisted of a surface vessel, a marine cable, and a towfish (Grosenbaugh, 2007; Huang, 1994; Park et al., 2003; Vaz and Patel, 1995). Because a marine cable exhibits highly nonlinear characteristics under water, analysis of marine cable dynamics has typically relied on numerical methods. In addition, the highly nonlinear motion of a marine cable can cause coupled motion of the towfish, add to the towfish's own nonlinear motion. A few studies have examined ways to control the motion of towfish, using devices such as a nonlinear adaptive controller (Curado et al., 2010). For analysis of the motion of marine cables, the lumped mass approximation method (Buckham et al., 2003; Kamman and Nguyen, 1990; Kamman and Huston, 2001) and classical cable theory based on the finite element method (Park et al., 2003; Wu and Chwang, 2001; Yuan et al., 2013) have usually been employed. The lumped mass approximation method assumes that the mass is concentrated at a nodal point and that the cable segment is a bar element. The great advantage of this method is its ease of implementation. The disadvantage of this method is that it cannot take into consideration bending deformation of the cable element. To address this limitation of the lumped mass approximation method, classical cable theory based on the finite element method can be applied. This approach can reveal a cable during motion. However, this approach requires dividing the cable into many segments to obtain accurate simulation result (Park et al., 2003). Another method for modeling cable dynamics

Corresponding author: *Nakwan Kim*, e-mail: *nwkim@snu.ac.kr*

is the Absolute Nodal Coordinate Formulation (ANCF) method (Berzeri and Shabana, 2000; Gerstmayr and Shabana, 2006; Gerstmayr et al., 2013; Shabana and Yakoub, 2001; Shabana et al., 1998). Only a few studies have applied this method to the analysis of underwater cable dynamics (Kim et al., 2012; Takehara et al., 2011). This method was first proposed by Shabana et al (1998) and has since been developed further by other researchers (Yakoub and Shabana, 1999; 2001). The great advantage of the ANCF method is that it uses a constant mass matrix in the equation formulation. Furthermore, it can produce accurate results with fewer cable segments than can be produced using classical cable theory (Berzeri and Shabana, 2000).

However, in the systems previously studied, the motion of the surface vessel dominated the whole system. Therefore, it is not necessary to consider the interaction force between the mother ship and the subsea system-in other words, the interaction force is negligible. However, in the case of a semi-submersible Autonomous Underwater Vehicle (AUV) system, the towing vehicle and the towfish are comparable in size, and the motion of the cable can affect the whole system, so we need to model the motion of the system as a multi-body system (Buckham et al, 2003). Semi-submersible AUV systems usually consist of three components: the towing vehicle, the towing cable, and the towfish (see Fig. 1). The towing vehicle is usually operated near the water surface (at a depth of approximately 3 to 5 meters), and 70-80% of the body is submerged in water. The main mission of the towing vehicle is to drive the towing cable and towfish. The towing cable connects the two vehicles, and the towfish explores the underwater environment. Because the towing vehicle is powered by an internal combustion engine, it is constrained to operate at depths that do not exceed 5 meters. Because the towfish has no self-propulsion, analyzing the cable motion is very important to controlling the towfish motion. Buckham et al. (2003) conducted dynamics modeling of such a system. However, in the proposed model, the cable dynamics were based on lumped mass approximation, which may lead to considerable modeling uncertainty.

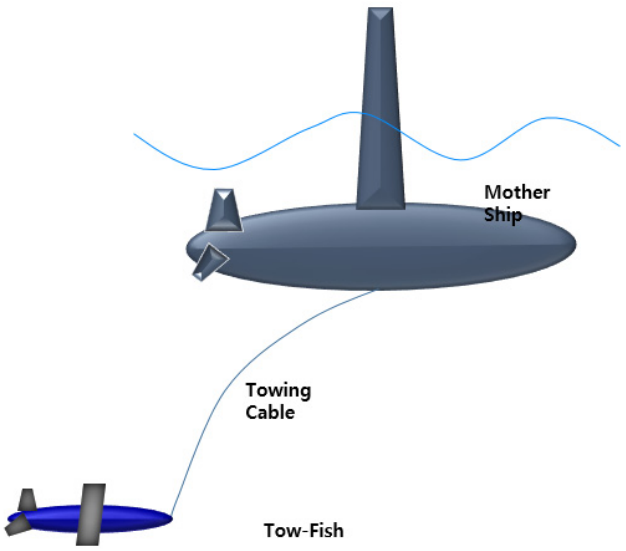

Fig. 1 Illustration of semi-submersible AUV.

This paper presents an approach to multi-body dynamics modeling of a semi-submersible system. The towing vehicle and towfish are modeled using 6-DOF rigid body dynamics. Because the towing cable can experience large deformations and displacements, its dynamics are modeled using the ANCF method. Considering the fact that the cable element has no signify-cant effect on torsional motion, we can formulate the cable using a lower-order cable element (Gerstmayr and Shabana, 2006), and doing so contributes to the computational efficiency of the model. This paper is organized as follows. The first section presents a brief review of the ANCF method and describes how an external force, including a hydrodynamic force, can be imposed on the cable dynamics. The second section presents the vehicle dynamics and the interaction force between the ve-hicles and the cable. The third section explains the computer implementation scheme used to solve the nonlinear equation for the system dynamics. The fourth section presents the steps in the numerical simulation process. The fifth section presents a few simple numerical simulations and discussion of the results obtained. Finally, the sixth section presents a summary of the research and the main conclusions drawn from the results.

CABLE MODELING

In a semi-submersible AUV system, the towing cable connects the towing vehicle and towfish and tows the towfish. Because the cable is a flexible body and can experience large deformations, depending on the motion of the towing vehicle and towfish, it is reasonable to model the cable using ANCF. This modeling approach can model large deformations and large rotations. In this formulation, the cable element is represented by a global position vector and a slope vector in absolute nodal coordinates, not a Euler angle, taking advantage of a constant mass matrix. In many cable element problems, the torsional stiffness has no significant effect (Gerstmayr and Shabana, 2006), and it is reasonable to model the cable as a lower-order cable element and thereby improve the calculation time. In a lower-order cable element based on ANCF, the nodal point of the element is composed of one position vector and one slope vector, obtained by differentiation with respect to the element center line. Fig. 2 illustrates the cable element representation.

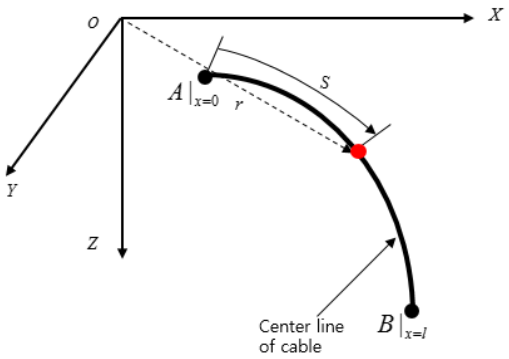

Fig. 2 Cable element representation.

Governing equation of motion of towing cable

As mentioned in the previous section, the nodal point of the cable element in three-dimensional space is defined by position vector and slope vector, as shown in Eq. (1):

$$\begin{aligned}
&\vec{e} = [e_1, e_2, e_3, e_4, e_5, e_6, e_7, e_8, e_9, e_{10}, e_{11}, e_{12}] \\
&e_1 = r_X|_{x=0}, e_2 = r_Y|_{x=0}, e_3 = r_Z|_{x=0}, e_4 = \left.\frac{\partial r_X}{\partial x}\right|_{x=0}, e_5 = \left.\frac{\partial r_Y}{\partial x}\right|_{x=0}, e_6 = \left.\frac{\partial r_Z}{\partial x}\right|_{x=0} \\
&e_7 = r_X|_{x=l}, e_8 = r_Y|_{x=l}, e_9 = r_Z|_{x=l}, e_{10} = \left.\frac{\partial r_X}{\partial x}\right|_{x=l}, e_{11} = \left.\frac{\partial r_Y}{\partial x}\right|_{x=l}, e_{12} = \left.\frac{\partial r_Z}{\partial x}\right|_{x=l}
\end{aligned} \tag{1}$$

where r_i $(i = X, \mathrm{Y}, \mathrm{Z})$ is the position vector of the nodal point and other components of the partial derivative of each positional vector with respect to the cable center line, l is the length of cable segment, and x is the arc-length coordinate of an arbitrary point on the undeformed cable element. The global position vector in an arbitrary cable element can be expressed as shown in Eq. (2):

$$\vec{r} = [r_X \; r_Y \; r_Z]^T = S\vec{e} \tag{2}$$

where S is a global shape function that is based on a cubic spline interpolation function and is an isoparametric function. This shape function can be expressed as shown in Eq. (3):

$$S = [S_1 I \; S_2 I \; S_3 I \; S_4 I] \tag{3}$$

where I is a 3×3 identity matrix and the polynomial function element S_i $(i = 1, 2, 3, 4)$ is as shown in Eq. (4):

$$\begin{aligned} S_1 &= 1-3\xi^2+2\xi^3 \qquad S_2 = l(\xi-2\xi^2+\xi^3) \\ S_3 &= 3\xi^2-2\xi^3 \qquad S_4 = l(\xi^3-\xi^2) \end{aligned} \tag{4}$$

where ξ is a nondimensional quantity defined as $\xi = x/l$. The value of this quantity ranges between zero and one.

The generalized mass matrix of the cable element can be derived from a kinetic energy formulation. The kinetic energy of the cable element is expressed as $T = 1/2\int_V \rho \dot{\vec{r}}^T \dot{\vec{r}} dV$. Because the positional vector is expressed as shown in Eq. (2), the generalized velocity vector can be expressed as shown in Eq. (5)

$$\dot{\vec{r}} = S\dot{\vec{e}} \tag{5}$$

Therefore, the kinetic energy of the cable element can be expressed as shown in Eq. (6):

$$T = \frac{1}{2}\int_V \rho \dot{\vec{r}}^T \dot{\vec{r}} dV = \frac{1}{2}\dot{\vec{e}}^T (\int_V \rho S^T S dV)\dot{\vec{e}} = \frac{1}{2}\dot{\vec{e}}^T M \dot{\vec{e}} \tag{6}$$

The generalized mass matrix of the cable element is as shown in Eq. (7):

$$M = \int_V \rho S^T S dV \tag{7}$$

where ρ is the density of the cable element and V is the volume of the cable element. Note that, in this formulation, the mass matrix remains constant.

Internal force

Because the cable element can experience large deformations and displacement, we need to consider elastic forces. As discussed in Section 2, in the case of a cable element, the torsional effect is not significant, and we need only consider elastic axial and bending force effects. These elastic forces can be derived from the strain energy of the cable element, which is expressed as shown in Eq. (8):

$$U = U_a + U_b = \frac{1}{2}\int_l (EA\varepsilon^2 + EI\kappa^2) dx \tag{8}$$

where U_a is the axial strain energy, U_b is the bending strain energy, ε is the axial strain, and κ is the curvature due to bending of the cable. Because the elastic force can be derived from the partial derivative of the strain energy with respect to the position vector, the elastic force component can be written as shown in Eq. (9):

$$F_{elastic} = F_a + F_b = \frac{\partial}{\partial \vec{e}}\int_l EA\varepsilon^2 dx + \frac{\partial}{\partial \vec{e}}\int_l EI\kappa^2 dx = K_a \vec{e} + K_b \vec{e} \tag{9}$$

where K_a is the axial stiffness matrix and K_b is the bending stiffness matrix. We then need to express ε and κ as functions of absolute nodal coordinates. Using Green's strain tensor, ε can be expressed as shown in Eq. (10):

$$\varepsilon = \frac{1}{2}\left(\frac{\partial \vec{r}}{\partial x}^T \frac{\partial \vec{r}}{\partial x} - 1\right) \tag{10}$$

We also define the following matrix: $S_l = S'^T S' = \frac{1}{l^2} S_\xi{}^T S_\xi$, where $S' = \frac{\partial S}{\partial x}$, $S_\xi = \frac{\partial S}{\partial \xi}$. Since $\vec{r} = S\vec{e}$ and $\partial \vec{r} / \partial x = (\partial S / \partial x)\vec{e}$, then $\varepsilon = 1/2(e^T S_l e - 1)$. Therefore, the axial stiffness matrix can be expressed as shown in Eq. (11):

$$K_a = \int_l EA\varepsilon_l S_l dx = \frac{1}{2}\int_l EA(\vec{e}S_l\vec{e} - 1)S_l dx \tag{11}$$

Note that stiffness matrix of the axial effect is composed of nodal coordinates $\vec{e}$, and the nonlinear effect arises.

The stiffness matrix for the bending effect can be derived from the curvature definition. The curvature is defined as the magnitude of the normal vector of the deformed shape, $\kappa = |r_{ss}|$. By the chain rule, $r_s = \partial r / \partial s = \partial r / \partial x \cdot \partial x / \partial s$, and $r_s = r_x(\partial x / \partial s) = r_x / |r_x|$. The curvature corresponding to small axial deformation can be expressed as shown in Eq. (12):

$$\kappa = \left| \frac{\partial r}{\partial x^2} \right| = \vec{e}^T S''^T S'' \vec{e} \tag{12}$$

Therefore, the stiffness matrix for bending effect is as shown in Eq. (13):

$$K_b = \int_l EIS''^T S'' dx \tag{13}$$

External force

The external forces acting on cable during its motion are the gravity force, buoyancy force, drag force, and force due to added mass. The external force can be calculated from the virtual work principle, as shown in Eq. (14):

$$\begin{aligned} &F^T \delta r = F^T S \delta e = Q_e \delta e \\ &\therefore Q_e = F^T S \end{aligned} \tag{14}$$

where Q_e is the generalized external force vector in ANCF and F is the force vector in global coordinates. Using this formulation, the generalized gravity force can be expressed as shown in Eq. (15):

$$Q_{Gravity} = \int_V [0 \ 0 \ \rho_c g] S dV \tag{15}$$

where ρ_c is the density of the cable material and g is gravitational acceleration. The buoyancy force can be derived as in Eq. (16):

$$Q_{Buoyancy} = \int_V [0 \ 0 \ -\rho g] S dV \tag{16}$$

Because the towing cable is moving in water, hydrodynamic forces need to be considered. In this case, we consider the drag force and the force due to added mass. The drag force is composed of two components: the normal-direction drag force and the tangential drag force.

The drag forces in the normal direction and the tangential direction at an arbitrary point on the cable element can be written as shown in Eq. (17):

$$F_{Dn} = -\frac{1}{2} C_{Dn} \rho_w d \,|\vec{V}_n|\, \vec{V}_n$$
$$F_{Dt} = -\frac{s_c}{d} \mu \vec{V}_t Nu(Rn) \tag{17}$$

where F_{Dn} is the normal-direction drag force per unit length; F_{Dt} is the tangential-direction drag force per unit length; C_{Dn} is the drag coefficient in the normal direction; $Nu(Rn)$ is the Nusselt number, which is a function of the Reynolds number; ρ_w is the density of water; d is the diameter of the cable element; s_c is the circumference of the cable cross section; $\vec{V}_n$ is the normal-direction velocity; $\vec{V}_t$ is the tangential velocity; and μ is the dynamic viscosity of water. The drag coefficient in the normal direction (Choc and Casarella, 1971) is expressed in terms of the Reynolds number, as shown in Eq. (18):

$$C_{Dn} = \frac{8\pi}{RnS_d}(1 - 0.87S^{-2}) \quad (0 < Rn \le 1)$$
$$C_{Dn} = 1.45 + 8.55Rn^{-0.9} \quad (1 < Rn < 30)$$
$$C_{Dn} = 1.1 + 4Rn^{-0.5} \quad (30 \le Rn \le 10^5) \tag{18}$$

where Rn is the Reynolds number and S_d is defined as $S_d = -0.07721 + \ln(8Rn^{-1})$.

For the tangential drag force, the relation between the average Nusselt number and the Reynolds number given by (Choc and Casarella, 1971) is defined as shown in Eq. (19):

$$Nu(Rn) = 0.55Rn^{1/2} + 0.084Rn^{2/3} \tag{19}$$

Using the vector relation illustrated in Fig. 3, the tangential velocity and the normal velocity vector can be calculated as show in Eq. (20):

$$\vec{V}_n = \vec{V} - (\vec{V} \cdot \vec{a})\vec{a}$$
$$\vec{V}_t = (\vec{V} \cdot \vec{a})\vec{a} \tag{20}$$

where $\vec{V}$ is the total velocity vector of the cable element and $\vec{a}$ is the normalized tangential vector at an arbitrary point on the cable element. The drag force on the cable can be formulated as shown in Eq. (21):

$$\vec{V} \cdot \vec{a}\, Q_{Drag} = \int_V F_{Dn}{}^T S dV + \int_V F_{Dt}{}^T S dV \tag{21}$$

The last component of external force on the cable is the force due to added mass. We assume the force acts in the normal direction. The acceleration in the normal direction can be calculated as shown in Eq. (22):

$$\dot{\vec{V}}_n = \dot{\vec{V}} - (\dot{\vec{V}} \cdot \vec{a})\vec{a} \tag{22}$$

where $\dot{\vec{V}}$ is the total acceleration. The force due to added mass can be written as shown in Eq. (23):

$$Q_{Ad} = -\int_V \rho_w \dot{\vec{V}}_n S dV \tag{23}$$

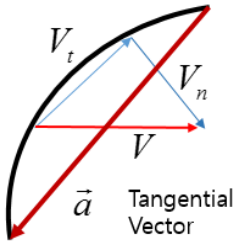

Fig. 3 Drag force description.

Constraints

In this system, we assume that the connecting parts between the vehicles and the cable are revolute joints. This type of joint only constrains the translational position. Therefore, the constraint equation for the connections between the vehicles and the cable can be written as shown below:

$$\begin{aligned}\Phi(e^m, e^{c1}) &= r^m - r^{c1} = S^m e^m - S^{c1} e^{c1} = 0 \\ \Phi(e^t, e^{cn}) &= r^t - r^{cn} = S^t e^t - S^{cn} e^{cn} = 0\end{aligned} \tag{24}$$

The first line of Eq. (24) is the constraint equation for the connection between the towing vehicle and the tow cable, and the second line is the constraint equation for the connection between the towfish and the towing cable. In these equations, e^m is the position of the towing vehicle in the global coordinate system, e^{c1} is the position vector of the first segment of the towing cable, e^t is the position of the towfish, and e^{cn} is the position vector of the n^{th} element (the cable is divided into n segments). This constraint can be interpreted as the boundary condition.

Overall equation of motion of cable

Integrating the force effects on cable, the overall equation of motion can be expressed as shown in Eq. (25):

$$M\ddot{\vec{e}} + K(\vec{e})\vec{e} = Q_{Drag} + Q_{Ad} + Q_{Gravity} + Q_{Buoyancy} \tag{25}$$

where $Q_{Buoyancy}$ is the buoyancy force. To impose the constraint equation and the interaction forces between the vehicle and cable, we employ a Lagrange multiplier. The overall equation of motion is as shown in Eq. (26):

$$\begin{bmatrix} M & \Phi_e^T \\ \Phi_e & 0 \end{bmatrix} \begin{bmatrix} \ddot{\vec{e}} \\ \lambda \end{bmatrix} = \begin{bmatrix} Q_q \\ \gamma \end{bmatrix} \tag{26}$$

where λ is the Lagrange multiplier, which can be interpreted as the interaction between the cable and a vehicle; Φ_e is the Jacobian matrix of constraints; γ is the matrix of acceleration-level kinematic constraints, which is defined as $\Phi_e \ddot{e} = -\Phi_{tt} - (\Phi_e \dot{\vec{e}})_e \dot{\vec{e}} - 2\Phi_{et}\dot{\vec{e}} \equiv \gamma$; and Q_q is the matrix of elastic forces and external forces. To obtain a stable solution, this algebraic equation is solved using the implicit Newmark integration method.

VEHICLE MODELING

The vehicles (the towing vehicle and the towfish) experience little deformation. Therefore, we formulate the motion of these vehicles using a 6-DOF rigid body model. To describe rigid body motion, two coordinate systems need to be

defined: the global coordinate system and the body fixed frame. Fig. 4 shows the coordinate systems used for the vehicle modeling.

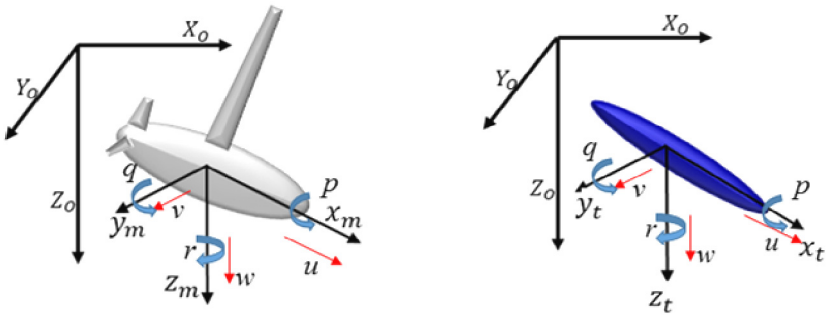

(a) Towing vehicle. (b) Tow-fish.

Fig. 4 Coordinate systems of vehicles.

6-DOF equation of motion of vehicle

Based on Newton's second law, Kirchhoff's equation of motion in the body fixed frame of the towing vehicle and the towfish can be written as shown in Eqs. (27) and (28):

$$\begin{aligned}
&m_m[\dot{u}-vr+wq-x_{Gm}(q^2+r^2)+y_{Gm}(pq-\dot{r})+z_{Gm}(pr+\dot{q})]=X_{hyd}+X_{prop}+X_{\text{int}}\\
&m_m[\dot{v}-wp+ur-y_{Gm}(r^2+p^2)+z_{Gm}(qr-\dot{p})+x_{Gm}(pq+\dot{r})]=Y_{hyd}+Y_{prop}+Y_{\text{int}}\\
&m_m[\dot{w}-uq+vp-z_{Gm}(p^2+q^2)+x_{Gm}(rp+\dot{q})+y_{Gm}(rq+\dot{p})]=Z_{hyd}+Z_{prop}+Z_{\text{int}}\\
&I_{xm}\dot{p}+(I_{zm}-I_{ym})qr+m_m[y_{Gm}(\dot{w}-uq+vp)-z_{Gm}(\dot{v}-wp+ur)]=K_{hyd}+K_{prop}+K_{\text{int}}\\
&I_{ym}\dot{q}+(I_{xm}-I_{zm})rp+m_m[z_{Gm}(\dot{u}-vr+wq)-x_{Gm}(\dot{w}-uq+vp)]=M_{hyd}+M_{prop}+M_{\text{int}}\\
&I_{zm}\dot{r}+(I_{ym}-I_{xm})pq+m_m[x_{Gm}(\dot{v}-wp+ur)-y_{Gm}(\dot{u}-vr+wp)]=N_{hyd}+N_{prop}+N_{\text{int}}
\end{aligned} \tag{27}$$

$$\begin{aligned}
&m_t[\dot{u}-vr+wq-x_{Gt}(q^2+r^2)+y_{Gt}(pq-\dot{r})+z_{Gt}(pr+\dot{q})]=X_{hyd}+X_{\text{int}}\\
&m_t[\dot{v}-wp+ur-y_{Gt}(r^2+p^2)+z_{Gt}(qr-\dot{p})+x_{Gt}(pq+\dot{r})]=Y_{hyd}+Y_{\text{int}}\\
&m_t[\dot{w}-uq+vp-z_{Gt}(p^2+q^2)+x_{Gt}(rp+\dot{q})+y_{Gt}(rq+\dot{p})]=Z_{hyd}+Z_{\text{int}}\\
&I_{xt}\dot{p}+(I_{zt}-I_{yt})qr+m_t[y_{Gt}(\dot{w}-uq+vp)-z_{Gt}(\dot{v}-wp+ur)]=K_{hyd}+K_{\text{int}}\\
&I_{yt}\dot{q}+(I_{xt}-I_{zt})rp+m_t[z_{Gt}(\dot{u}-vr+wq)-x_{Gt}(\dot{w}-uq+vp)]=M_{hyd}+M_{\text{int}}\\
&I_{zt}\dot{r}+(I_{yt}-I_{xt})pq+m_t[x_{Gt}(\dot{v}-wp+ur)-y_{Gt}(\dot{u}-vr+wp)]=N_{hyd}+N_{\text{int}}
\end{aligned} \tag{28}$$

Eq. (27) is the equation of motion of the towing vehicle, and Eq. (28) is the equation of motion of the towfish. In Eq. (27) and (28), $[u,v,w]^T$ is surge, sway and heave directional linear velocity in body fixed frame, and $[p,q,r]^T$ is roll, pitch and yaw angular velocity in body fixed frame. $[x_{Gm},y_{Gm},z_{Gm}]^T$ and $[x_{Gt},y_{Gt},z_{Gt}]^T$ are the position of center of gravity of towing vehicle and towfish in its body fixed frame. The subscript *int* refers to the interaction force, the subscript *hyd* refers to the hydrodynamic force, and the subscript *prop* refers to the propulsion force. Because the towfish has no self-propulsion, the propulsion force term is absent in the right-hand side of the equation of motion. As mentioned earlier, the equation of motion of vehicles is described in the fixed-body frame. Therefore, we need to transform the frame.

Interaction force and moment between towing vehicle and towing cable

The interaction between the cable and the towing vehicle is assumed to affect the thrust force of the towing vehicle. As Fig.

5 shows, once the equation of the towing vehicle is solved, the boundary condition of the cable is determined. The interaction force acts on the motion of the towing vehicle. As shown in Eq. (26), λ, the Lagrange multiplier, can be interpreted as the interaction force. Therefore, the thrust force and moment of towing vehicle can be written as shown in Eq. (29):

$$\begin{bmatrix} X_{prop}+X_{\text{int}} \\ Y_{prop}+Y_{\text{int}} \\ Z_{prop}+Z_{\text{int}} \end{bmatrix} = \begin{bmatrix} X_{prop} \\ Y_{prop} \\ Z_{prop} \end{bmatrix} + R_{IV}{}^{T} \begin{bmatrix} \lambda_1 \\ \lambda_2 \\ \lambda_3 \end{bmatrix}$$
$$\begin{bmatrix} K_{prop}+K_{\text{int}} \\ M_{prop}+M_{\text{int}} \\ N_{prop}+N_{\text{int}} \end{bmatrix} = \begin{bmatrix} K_{prop} \\ M_{prop} \\ N_{prop} \end{bmatrix} + r_{attatch} \times R_{IV}{}^{T} \begin{bmatrix} \lambda_1 \\ \lambda_2 \\ \lambda_3 \end{bmatrix} \tag{29}$$

where $R_{IV}{}^{T}$ is the transformation matrix between the fixed-body coordinates and the global coordinates for the towing vehicle, the subscript *prop* refers to the thrust force and moment without the cable, and $r_{attatch}$ is the position vector of the cable attached to the towing vehicle in the body fixed coordinate. When $r_{attatch}$ is not zero, we need to consider the moment due to the cable, expressed as the cross product of $r_{attatch}$ and the interaction force.

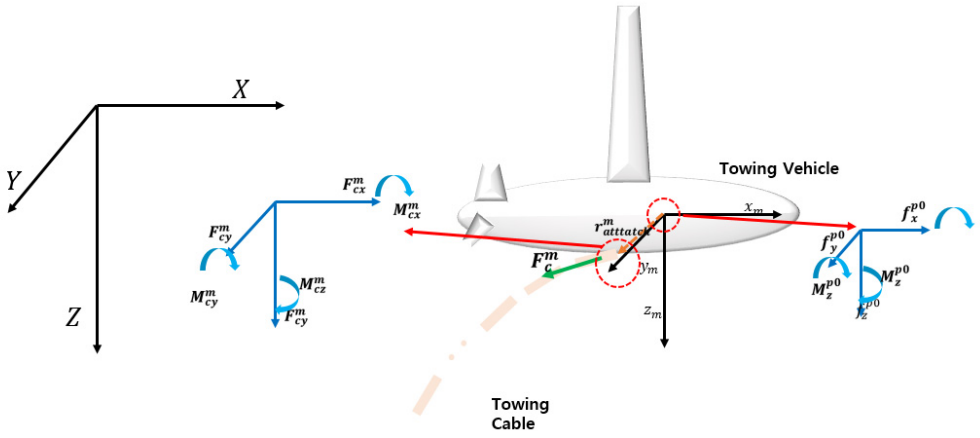

Fig. 5 Illustration of interaction between towing vehicle and towing cable.

Interaction force and moment between towing cable and towfish

The interaction force between the towfish and the towing cable is almost same as that between the towing vehicle and the towing cable. The one difference is that the towfish has no thrust of its own. The interaction force acting on the towfish is an external force. Thus, we can write the thrust of the towfish as shown in Eq. (30):

$$\begin{bmatrix} X_{\text{int}} \\ Y_{\text{int}} \\ Z_{\text{int}} \end{bmatrix} = R_{IV}{}^{T} \begin{bmatrix} \lambda_4 \\ \lambda_5 \\ \lambda_6 \end{bmatrix}$$
$$\begin{bmatrix} K_{\text{int}} \\ M_{\text{int}} \\ N_{\text{int}} \end{bmatrix} = r_{attatch} \times R_{IV}{}^{T} \begin{bmatrix} \lambda_4 \\ \lambda_5 \\ \lambda_6 \end{bmatrix} \tag{30}$$

Because the towfish has no self-propulsion force and moment, the position of the towing cable attached to the towfish plays an important role in towfish motion.

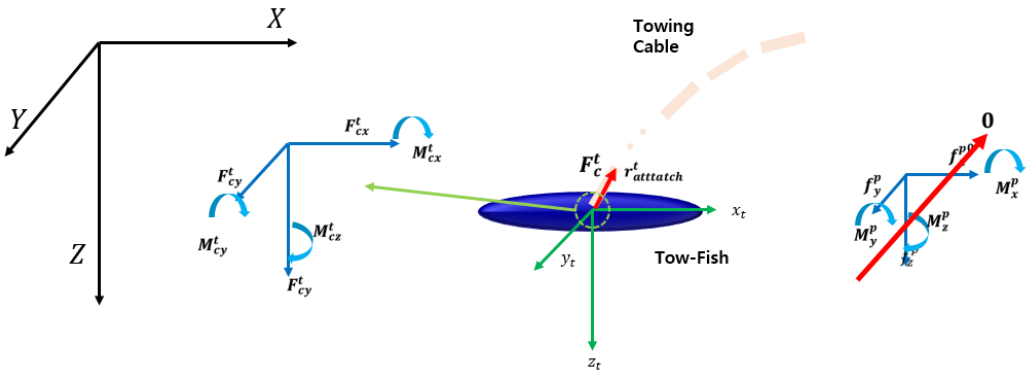

Fig. 6 Illustration of interaction between towfish and towing cable.

SIMULAITON PROCEDURE

Fig. 7 illustrates the simulation procedure. The steps in the simulation procedure are as follows:

Step 1. Initialize the parameters, position, velocity, acceleration, and interaction force.

Step 2. Solve the equation of motion for the towing vehicle and the towfish.

Step 3. Using the results of step 2 as boundary conditions for the cable equation, solve the cable dynamics equation using the implicit Newmark method.

Step 4. Update state of vehicles and cable state.

Step 5. Iterate steps 2-4 until the simulation termination time is reached.

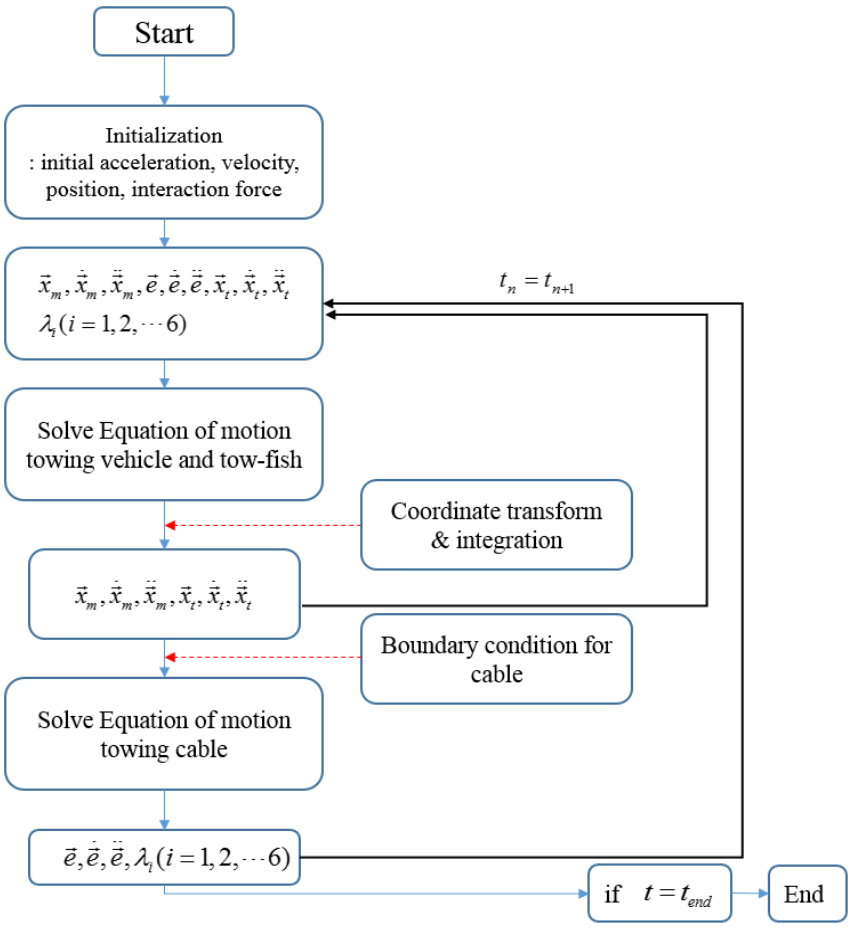

Fig. 7 Simulation procedure.

NUMERICAL SIMULATION

To evaluate the validity of the proposed modeling approach, two numerical simulations are conducted. The first simulation case is forward running with constant propeller thrust of the towing vehicle. The second case is a turning test with a 20 *degree* rudder deflection angle of the towing vehicle at steady-state forward running. The first case allows us to examine the behavior of the cable, the towfish, and the towing vehicle during the acceleration and the steady-state behavior of the system. The second case allows us to examine the system's behavior during a turning motion. In the simulation, the initial conditions of the towing vehicle are zero velocity and acceleration and a 3.5 *m* depth. The cable length is set to 200 *m*, and the towfish has the same velocity and acceleration as the towing vehicle and a 203.5 *m* depth. The cable is attached to the bow of the towfish to provide stability in forward running, and on the towing vehicle, the cable is attached at the center of gravity. As shown in Fig. 1, the towing vehicle has three fins such as two elevators and one rudder, and the tow fish has main wings, two elevators and one rudder. The towing vehicle and the towfish have a torpedo-type body and employ the hydrodynamic coefficients of ISiMI (Jun et al., 2009) for bodies and fins and the coefficients of SNU Glider (Seo, 2009) for the main wings of the towfish. The cable material density is set to 1300 kg/m^3, and the diameter of the circular cross section is set to 4.1 cm . The parameters used for simulation are given in Table 1.

Table1 Parameters for computation.

Item	Value	Unit
Density of cable	1300	kg / m^3
Length of cable	200	m
Young's modulus of cable	7×10^8	N / m^2
Diameter of cable	0.041	m
Length of towing vehicle	8.2	m
Mass of towing vehicle	6950	kg
Moment of inertia of towing vehicle	[397.04, 3969.8, 3069.1]	$kg \cdot m^4$
Center of mass of towing vehicle	[0,0,0.2]	m
Length of towfish	3.3	m
Mass of towfish	416	kg
Moment of inertia of towfish	[28.64, 286.35, 301.47]	$kg \cdot m^4$
Center of mass of towfish	[1,0,0.12]	m

Case 1: Forward running

Figs. 8-13 illustrate the results of the first simulation case over a time period of 100 seconds. Fig. 8 shows the cable alignment every 15 seconds. In this figure, we can observe the cable shape during the transient interval. It is because the velocity of cable near the towing vehicle is faster than that of lower part. This can be seen in Fig. 8. Also, the cable lower bound is biased to rear. This is because the velocity of towfish is not in steady state and the cable end is biased to towfish position. After the transient interval, the shape of the cable is almost a straight line. This cable shape indicates that the forward running motion of the system entered a steady state. Figs. 9 and 10 show that the motion of system entered a steady state at approximately 50 seconds and that the steady-state surge velocity is 6 *m/s*. An interesting observation is that the towfish entered a steady state approximately 30 seconds later than the towing vehicle. The reason for this is that the towfish follows the towing vehicle and the towing cable; therefore the dynamics of the towing vehicle are transferred to the towfish with a time lag. Figs. 12 and 13 show that the interaction force is well reflected in system dynamics, and in the steady state, only the surge-directional interaction force remains. Based on the results of Case 1, we conclude that the dynamics modeling of the semi-submersible AUV system describes the behavior of the physical system well.

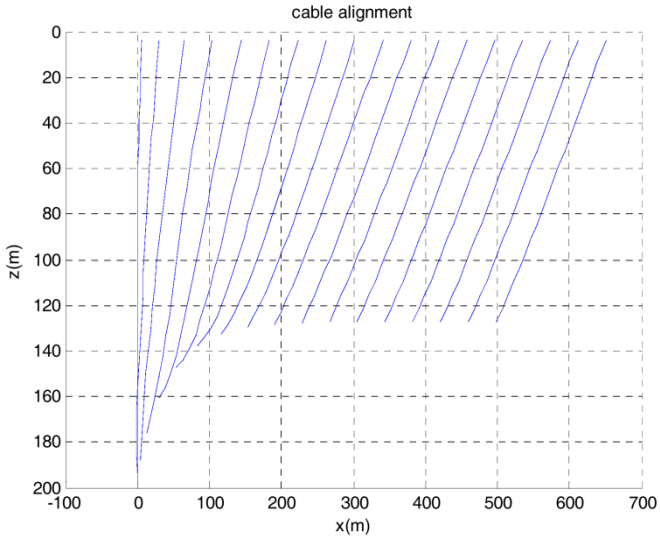

Fig. 8 Cable alignment: Case 1.

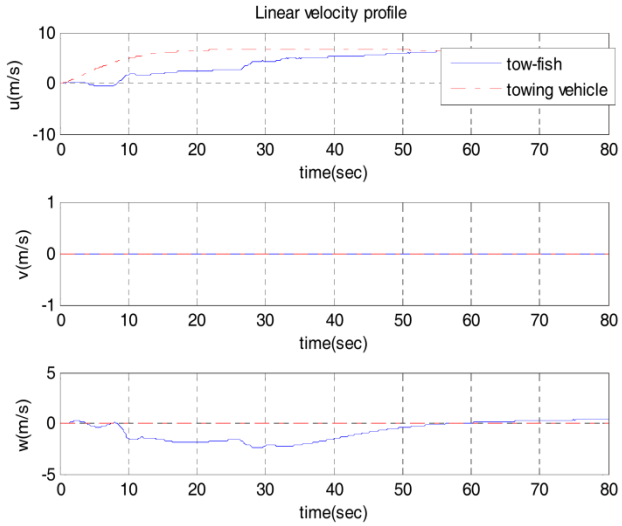

Fig. 9 Linear velocity profile: Case 1.

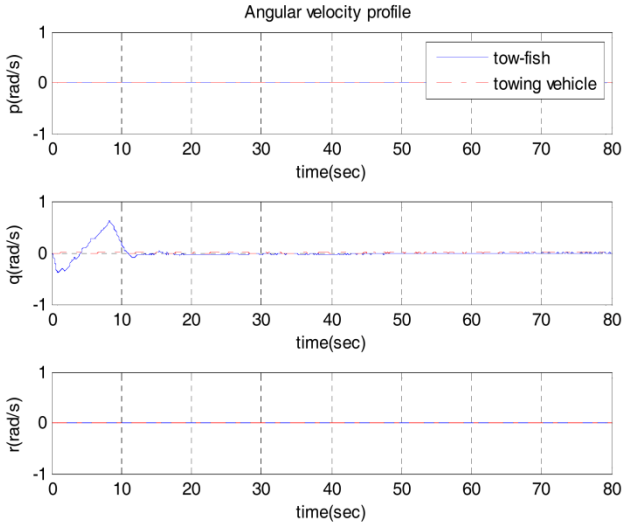

Fig. 10 Angular velocity profile: Case 1.

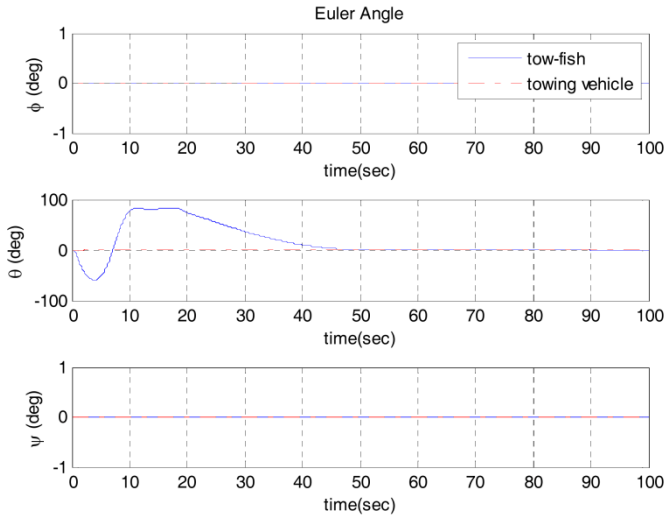

Fig. 11 Euler angle: Case 1.

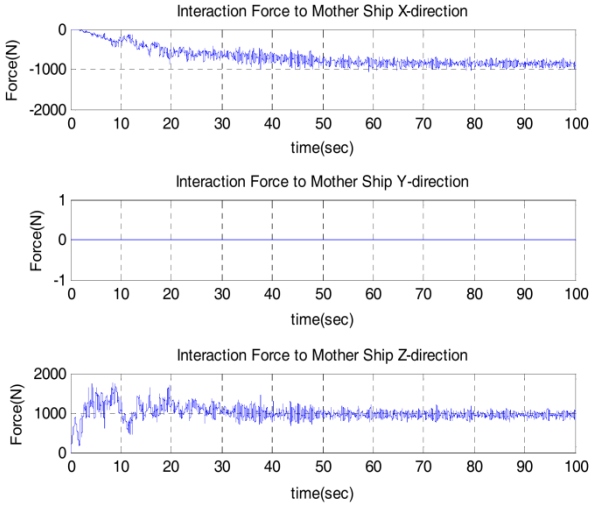

Fig. 12 Interaction force of towing vehicle: Case 1.

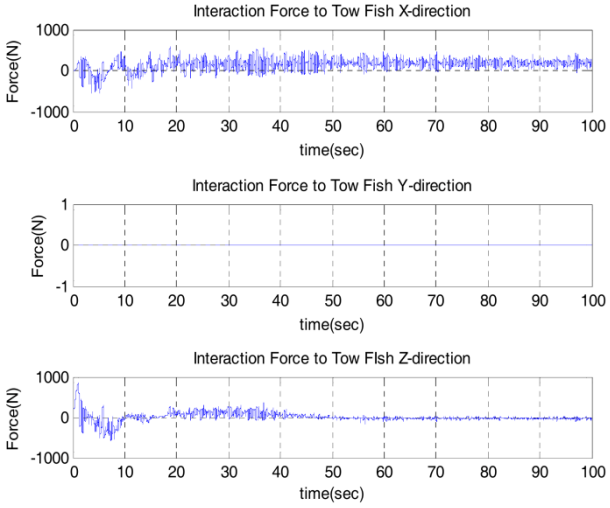

Fig. 13 Interaction force of towfish: Case 1.

Case 2: Turning behavior

This simulation is conducted to investigate the behavior of the system while executing a U turn. In the simulation, the initial motion is forward running for 55 seconds to allow the system to enter a steady state, and during the rest of the simulation time, a turning command with a 20-degree rudder deflection is applied. Once the yaw angle of the towing vehicle reached 170 degrees, the rudder is set back to a zero angle of deflection to make the towing vehicle execute a U-shaped turning motion. Figs. 14-20 show the results of the simulation. As Fig. 14 shows, the turning radii of the towing vehicle and the towfish are significantly different. The reason for this is that the turning motion of the towing vehicle is transferred to the towfish with a time lag, and the motion of the towing cable and the towfish have nonlinearity. The difference in the turning radius of the towing vehicle and that of the towfish is similar to that reported in Grosenbaugh (2007). Also the depth of the towfish increases during the turning motion and decreases after the turning motion. A comparison of the results obtained by Grosenbaugh (2007) and those obtained in this study suggests that the shape of the trajectory of the towfish is different from that of the tow vehicle because of the form of the towfish and its dynamics.

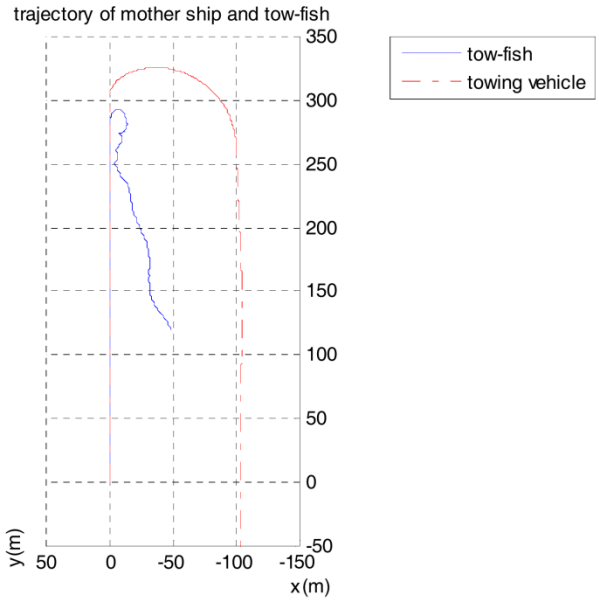

Fig. 14 Overview of trajectory of towing vehicle and towfish: Case 2.

In Grosenbaugh (2007), the towfish is a simple cylinder in shape, and in this study, a nonlinear equation of motion is applied to the towfish dynamics. Fig. 16 shows that the pitch angular velocity oscillated around approximately 80 seconds, and the same phenomenon is observed in Fig. 15 for the heave velocity. The behavior of the towfish provides a clue to the explanation of this phenomenon. Figs. 15-17 show that the velocity and Euler angle of the towfish exhibit different patterns from Case 1. A sudden increase (or decrease) in the velocity and Euler angle indicates that the towfish starts to turn after approximately 80 seconds. This suggests that the effect of the turning motion of the towfish is transferred to the towing vehicle, and the phenomena described above occur. In addition, we notice this effect in the interaction force between the vehicles and the cable, as shown in Figs. 18 and 19. The time lag to enter the steady state that is observed in the first simulation case is almost same as the time lag in the second simulation case. Another observation that we can make is that the overall motion of the towfish during a turning motion is very unstable. We may also need a proper controller to make the motion of the towfish stable.

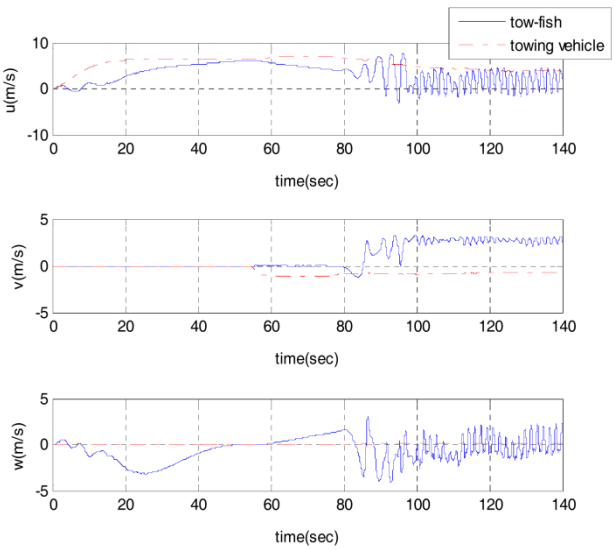

Fig. 15 Linear velocity profile: Case 2.

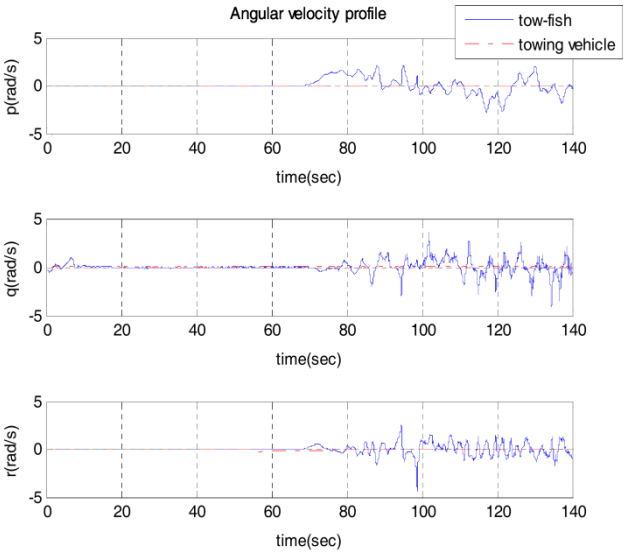

Fig. 16 Angular velocity profile: Case 2.

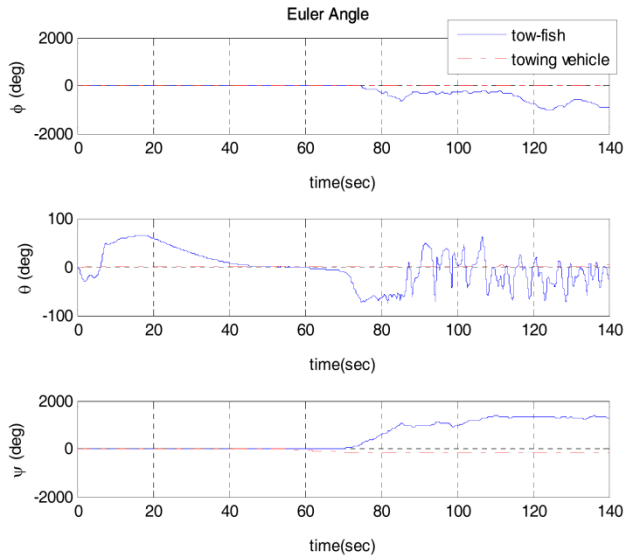

Fig. 17 Euler angle: Case 2.

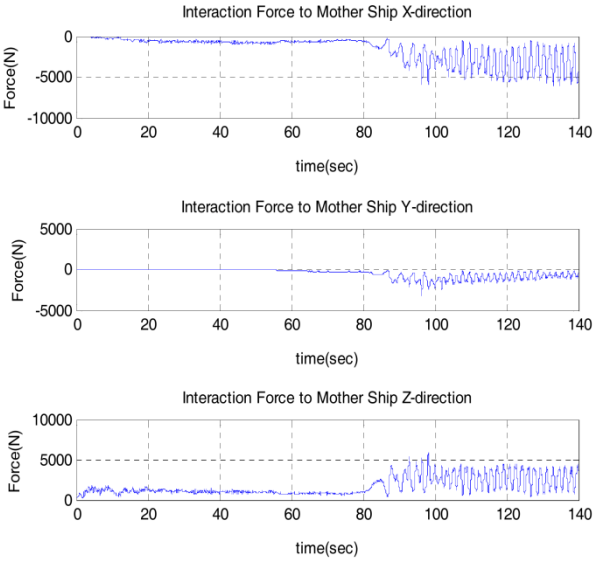

Fig. 18 Interaction force of towing vehicle: Case 2.

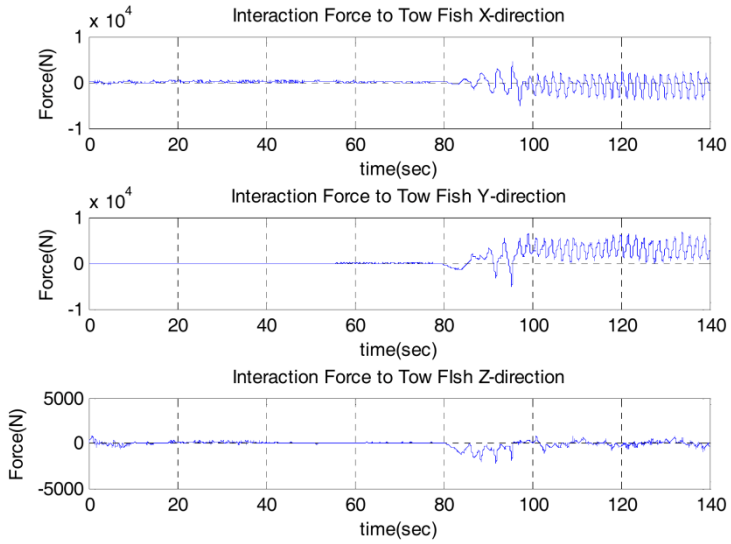

Fig. 19 Interaction force of towfish: Case 2.

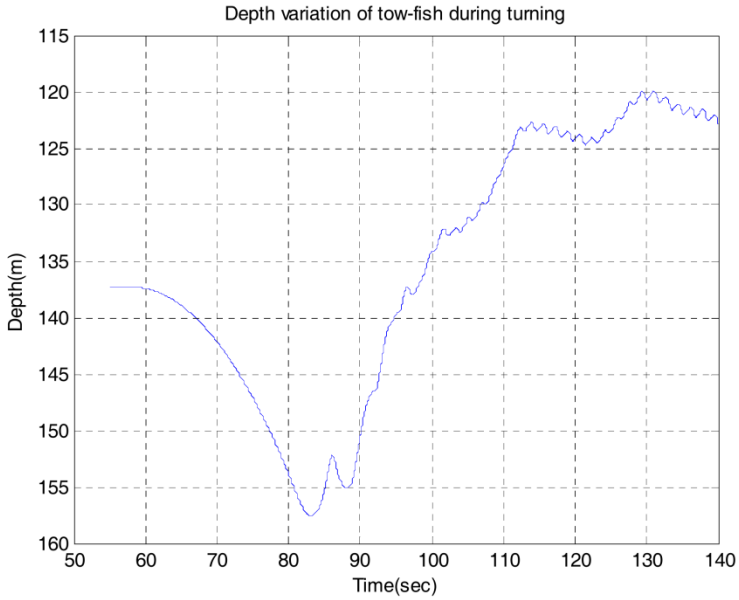

Fig. 20 Depth variation of towfish during turning motion.

CONCLUSIONS AND FUTURE WORK

This paper presents approach to modeling the dynamics of a semi-submergible AUV system with a towfish towed by an underwater cable. The towing vehicle and towfish are modeled using a 6-DOF rigid-body equation of motion, and the marine cable is modeled using ANCF to express the deformation of cable. In modeling the dynamics, hydrodynamic forces are applied to the system. To verify the completeness of the modeling approach, two numerical simulations are conducted. The first simulation case is a straight running situation, and the second is a U-turn motion. Based on the results, we can draw the following conclusions concerning the proposed modeling procedure for a semi-submersible AUV system.

1) The cable in the system can be modeled well using ANCF. This modeling approach for the cable takes into consideration the deformation of the cable and the interaction force between vehicles.
2) Hydrodynamic forces, drag forces, and forces due to added mass are applied to the cable element, and in the steady state, those external forces and the internal forces are in equilibrium.

3) In the first simulation case, the towfish motion is sufficiently stable, which suggests that the towfish can perform its mission well when moving without turning.
4) There is a time lag in the transfer of the effect of the motion of the towing vehicle to the towfish. The time lags are almost the same in the two simulations conducted.
5) The results of the turning simulation indicate that the towfish motion becomes less stable during turning, which suggests that it may need to be operated with a proper controller.
6) The results of the simulations for the modeled system compare well with the results of other studies; the overall motion of the modeled system agreed well in a physical sense with that observed in other studies.

ACKNOWLEDGMENT

This research was supported by Basic Science Research Program through the National Research Foundation of Korea (NRF) funded by the Ministry of Education, Science and Technology (NRF-2012R1A1A2008633).

REFERENCES

Berzeri, M. and Shabana, A.A., 2000. Development of simple models for the elastic forces in the absolute nodal co-ordinate formulation. *Journal of Sound and Vibration*, 235(4), pp.539-565.

Buckham, B., Nahon, M., Seto, M., Zhao, X. and Lambert, C., 2003. Dynamics and control of a towed underwater vehicle system, part I: model development. *Ocean Engineering*, 30(4), pp.453-470.

Choc, Y.I. and Casarella, M.J., 1971. Hydrodynamic resistance of towed cables. *Journal of Hydronautics*, *5*(4), pp.126-131.

Curado, T.F., Pedro, A.A. and Pascoal, A., 2010. Nonlinear adaptive control of an underwater towed vehicle. *Ocean Engineering*, 37(13), pp.1193-1220.

Gerstmayr, J. and Shabana, A.A., 2006. Analysis of thin beams and cables using the absolute nodal co-ordinate formulation. *Nonlinear Dynamics*, 45(1-2), pp.109-130.

Gerstmayr, J., Sugiyama, H. and Mikkola, A., 2013. Review on the absolute nodal coordinate formulation for large deformation analysis of multi-body systems. *Journal of Computational and Nonlinear Dynamics*, 8(3), pp.031016.

Grosenbaugh, M.A., 2007. Transient behavior of towed cable systems during ship turning maneuvers. *Ocean engineering*, 34(11), pp.1532-1542.

Huang, S., 1994. Dynamic analysis of three-dimensional marine cables. *Ocean Engineering*, 21(6), pp.587-605.

Jun, B.H., Park, J.Y., Lee, F.Y., Lee, P.M., Lee, C.M. and Oh, J.H., 2009. Development of the AUV 'ISiMI' and a free running test in an Ocean Engineering Basin. *Ocean engineering*, 36(1), pp.2-14.

Kamman, J.W. and Nguyen, T.C., 1990. *Modeling towed cable system dynamics (No. NCSC-TM-492-88)*. Panama City, FL: Naval Coastal Systems Center.

Kamman, J.W. and Huston, R.L., 2001. Multi-body dynamics modeling of variable length cable systems. *Multi-body System Dynamics*, *5*(3), pp.211-221.

Kim, K.W., Lee, J.W. and Yoo, W.S., 2012. The motion and deformation rate of a flexible hose connected to a mother ship. *Journal of mechanical science and technology*, 26(3), pp.703-710.

Park, H.I., Jung, D.H. and Koterayama, W., 2003. A numerical and experimental study on dynamics of a towed low tension cable. *Applied Ocean Research*, 25(5), pp.289-299.

Shabana, A.A. and Yakoub, R.Y., 2001. Three-dimensional absolute nodal coordinate formulation for beam elements: theory. *Journal of Mechanical Design*, 123(4), pp.606-613.

Shabana, A.A., Hussien, H.A. and Escalona, J.L., 1998. Application of the absolute nodal coordinate formulation to large rotation and large deformation problems. *Journal of Mechanical Design*, 120(2), pp.188-195.

Seo, D.C., 2009. *A study on the underwater glider design based on stability analysis and motion behavior*. Ph.D. Dissertation, Seoul National University.

Takehara, S., Terumichi, Y. and Sogabe, K., 2011. Motion of a submerged tether subject to large deformations and displacements. *Journal of System Design and Dynamics*, 5(2), pp.296-305.

Vaz, M.A. and Patel, M.H., 1995. Transient behaviour of towed marine cables in two dimensions. *Applied Ocean Research*, 17(3), pp.143-153.

Wu, J. and Chwang, A.T., 2001. Investigation on a two-part underwater manoeuvrable towed system. *Ocean Engineering*, 28(8), pp.1079-1096.

Yakoub, R.Y. and Shabana, A.A., 1999. Use of Cholesky coordinates and the absolute nodal coordinate formulation in the computer simulation of flexible multi-body systems. *Nonlinear Dynamics*, 20(3), pp.267-282.

Yakoub, R.Y. and Shabana, A.A., 2001. Three dimensional absolute nodal coordinate formulation for beam elements: implementation and applications. *Journal of Mechanical Design*, 123(4), pp.614-621.

Yuan, Z., Jin, L., Chi, W. and Tian, H., 2013. Finite difference method for solving the nonlinear dynamic equation of underwater towed system. *International Journal of Computational Methods*, 11(4), pp.1350060